ACCEPTED MANUSCRIPT
DOI of the published work: https://doi.org/10.1016/j.ijsolstr.2020.10.019
International Journal of Solids and Structures, Volumes 208–209, January 2021, Pages 1-12

The Octahedron family as a source of tensegrity families: the X-Octahedron family

Manuel Alejandro Fernández-Ruiz[a,*], Enrique Hernández-Montes[b], Luisa María Gil-Martín[c]

[a] Department of Industrial and Civil Engineering, University of Cádiz (UCA). Campus Bahía de Algeciras, Avda. Ramón Puyol, s/n. 11201 Algeciras (Cádiz), Spain. manuelalejandro.fernandez@uca.es.
*Corresponding author

[b] Department of Structural Mechanics, University of Granada (UGR). Campus Universitario de Fuentenueva s/n. 18072 Granada, Spain. emontes@ugr.es.

[c] Department of Structural Mechanics, University of Granada (UGR). Campus Universitario de Fuentenueva s/n. 18072 Granada, Spain. mlgil@ugr.es.

Abstract

A tensegrity family is a group of tensegrity structures that share a common connectivity pattern. The three first members of the Octahedron family are the octahedron, the expanded octahedron and the double-expanded octahedron. In this work a new family is presented: the X-Octahedron family. If in the elementary rhombic cells of the Octahedron family a diagonal cable is introduced then X-rhombic cells are obtained, resulting in tensegrity forms that belongs to the new family. Three members of the family have been obtained: the X-octahedron, the X-expanded octahedron and the X-double-expanded octahedron. Several element groupings have been considered in order to find new equilibrium shapes of the members of the new family. The values of the force:length ratios which satisfy the super-stability conditions have been computed analytically.

Keywords: Tensegrity; Octahedron family; X-Octahedron family; Analytical form-finding; Force density method.

1. Introduction

Tensegrity, a structure composed by pre-stressed pin-jointed compression (struts) and tension (cables) members that are self-equilibrated, was firstly introduced by Fuller (Fuller, 1975). Tensegrity structures have had a great development in the last years due to their unique mechanical and mathematical properties in comparison with conventional structural forms such as trusses and frames (Zhang and Ohsaki, 2015). In biology, the principles of tensegrity structures have been used in cells (Ingber, 2003, 1993) and tissues (Maina, 2007). In industrial and civil engineering tensegrity structures have a wide variety of applications such as deployable aerospace devices (Tibert and Pellegrino, 2002), robotic (Graells Rovira and Mirats Tur, 2009) and civil engineering works (Rhode-Barbarigos et al., 2010).

The two key aspects in the design of tensegrity structures are the self-equilibrium and the (super-)stability (Zhang and Ohsaki, 2015). The cables and struts of a tensegrity carry axial forces even when no external load is applied (self-stresses). The geometrical configuration and the prestress state of both cables and struts are interdependent with each other. This is the main difficulty in finding an equilibrium shape of a tensegrity. The problem of determining the self-equilibrated configuration is called form-finding. In (Tibert and Pellegrino, 2003) a review of form-finding methods of tensegrity structures is presented. The Force Density Method (FDM) is one of the most used form-finding methods of pin-jointed networks (Linkwitz and Schek, 1971; Schek, 1974). The equilibrium equations (which are highly nonlinear) are linearized introducing the concept of force:length ratio or force density q. The FDM has been widely used in

several form-finding methods of tensegrity structures (Tran and Lee, 2010; Vassart and Motro, 1999; Zhang and Ohsaki, 2006). The dynamic relaxation method introduced by Otter (Otter, 1965) has also been used in the form-finding problem of tensegrity structures (Bel Hadj Ali et al., 2011; Motro, 1984).

The existing form-finding methods can be classified into two categories: numerical and analytical. Numerical methods are used to solve the form-finding problem of complex tensegrity structures with a high number of members. In the literature there are many works related to numerical form-finding methods; examples of them can be seen in (Estrada et al., 2006; Masic et al., 2005; Tran and Lee, 2010; Zhang and Ohsaki, 2006). In (Feng and Guo, 2015), a numerical method is presented in which assumptions such as element lengths, initial nodal coordinates, material properties, structural symmetry and the positive semi-definiteness condition of the force density matrix are no longer necessary. (Micheletti and Williams, 2007) proposed another numerical method that can be applied to large tensegrity structures. Finally, in (Zhang and Ohsaki, 2013) the non-rigid-body motion analysis is presented, a numerical method based on the technique of singular value decomposition. On the other hand, analytical methods are usually used for simple tensegrities with a relatively small number of members or high symmetry. There are not so many works in the literature about analytical form-finding methods of tensegrity structures (Fernández-Ruiz et al., 2019a; Hernández-Montes et al., 2018; Vassart and Motro, 1999; Zhang et al., 2013). Analytical form-finding methods achieve the equilibrium shape through a symbolic analysis. In general, some symmetric properties of the resultant tensegrity are enforced in order to simplify the form-finding problem. In fact, symmetry has been a great source of new tensegrity forms (Estrada et al., 2005; Masic et al., 2005). In (J. Y. Zhang et al., 2009a, 2009b) analytical formulations of the equilibrium, force density and geometrical stiffness matrices for

prismatic tensegrity structures with dihedral symmetries were presented. Other source of tensegrity forms are the so-called "truncated regular polyhedral tensegrities", which are obtained from geometrical forms (Zhang et al., 2019, 2013, 2012; Zhang and Ohsaki, 2012). Analytical form-finding methods give a deep understanding of both the geometry and the self-stress state of the tensegrity while numerical methods only give a discrete solution of the self-equilibrium state.

The other key aspect in the design of tensegrity structures is the stability (Sultan et al., 2001). The super-stability is a robust stability criterion for tensegrity structures (Connelly, 1998; Zhang and Ohsaki, 2007). A tensegrity structure is said to be super-stable if it is always stable for any level of self-stress and material properties considered (Connelly, 1998; Zhang and Ohsaki, 2007). In super-stable tensegrities, an increase of the prestress of their members tend to stiffen them (Connelly and Back, 1998), which is an important property for the potential applications of tensegrities in both industrial and civil engineering.

A tensegrity family is defined as a group of tensegrity structures that share the same connectivity pattern (Fernández-Ruiz et al., 2019a). Each tensegrity has a position into the family in such a way that it has as folded forms all the lower members of the family. Folded forms are tensegrity structures where some nodes in the equilibrium shape share the same position in the space (Hernández-Montes et al., 2018). On the other hand, full forms are defined as tensegrity structures whose nodes in the equilibrium configuration have different coordinates (Hernández-Montes et al., 2018). The authors introduced in a previous work the Octahedron family (Fernández-Ruiz et al., 2019a), which is made up of the octahedron, the expanded octahedron and the double-expanded octahedron. In the form-finding process of these three tensegrities only two possible values of q were considered (i.e., one for cables and another one for struts). The possibility of

considering a higher number of possible values of q was studied in (Fernández-Ruiz et al., 2019b).

New tensegrity families can be obtained based on the Octahedron family. In (Fernández-Ruiz et al., 2020) authors presented the Z-Octahedron family. The Z-Octahedron family was obtained replacing the rhombic cells of the Octahedron family by Z-shaped cells. This design method is based on cell substitution (Feng et al., 2010; Zhang et al., 2013). Elementary cells are like tensegrity modules (Aloui et al., 2019; Nishimura and Murakami, 2001) which are used to construct tensegrity structures. This idea has been also used by (Aloui et al., 2018) for the generation of planar tensegrity structures inspired by the multiplication mechanisms of unicellular organisms.

In this work the Octahedron family is presented as a source of tensegrity families. A new tensegrity family is presented: the X-Octahedron family. This new family has been obtained replacing the elementary rhombic cells of the Octahedron family by X-rhombic cells (five cables and one strut). Unlike other sources of tensegrity structures based on symmetry and geometrical forms, in this work new tensegrity forms are obtained based on the connectivity pattern (topology) of the Octahedron family. Several element groupings have been considered in order to obtain different equilibrium configurations of the members of the X-Octahedron family.

2. Elementary cells for the construction of tensegrity structures: tensegrity families and truncated regular polyhedral tensegrities

Tensegrity structures can be obtained by different procedures. Among other methods, a tensegrity can be constructed based on the topology of its family as in (Fernández-Ruiz et al., 2019a) or by purely geometrical intuition based on truncated regular polyhedrons (Li et al., 2010; Zhang and Ohsaki, 2012; Zhang et al., 2013, 2012). Moreover, new

tensegrity forms can be obtained based on cell substitution (Feng et al., 2010; Fernández-Ruiz et al., 2020; Zhang et al., 2013).

2.1 Elementary cells

It is known that tensegrity structures can be constructed by assembling elementary cells (Li et al., 2010; Pugh, 1976). The elementary cells shown in Figure 1 are not tensegrity structures by themselves but they can be used to construct them. All the elementary cells considered in this work fulfills the condition proposed by Pugh in (Pugh, 1976): there is not any connection between two struts (i.e. each node is only connected to one strut). In the diamond pattern described in (Pugh, 1976) cables form diamonds or rhombic cells with a strut defining one diagonal (see Figure 1.a). On the other hand, in the zigzag pattern an opposite pair of cables of a diamond cell are removed while a new cable is added (Pugh, 1976) (see Z-shaped cell in Figure 1.b). Finally, a five-cable diamond cell is obtained by adding a diagonal cable to a diamond cell (Li et al., 2010) (see Figure 1.c). In this work, this elementary cell is called "X-diamond" or "X-rhombic".

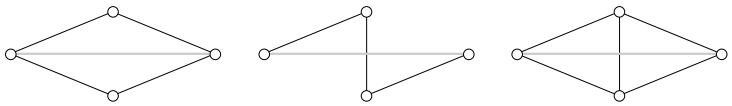

Figure 1. (a) Diamond or rhombic, (b) zigzag or Z-shaped and (c) X-diamond or X-rhombic elementary cells (black and grey lines correspond to cables and struts respectively).

2.2 Truncated regular polyhedral tensegrities

Truncated regular polyhedrons are a source of tensegrity structures called "truncated regular polyhedral tensegrities" (Zhang and Ohsaki, 2012; Zhang et al., 2013, 2012). These tensegrities are constructed following the procedure proposed by (Li et al., 2010), according to which the nodes of the truncated regular polyhedral tensegrities coincide with the vertices of the truncated polyhedron. Let us consider the truncated tetrahedron

shown in Figure 2.a as an example. The struts connect some vertices of the truncated tetrahedron following the indications proposed in (Li et al., 2010) (see grey lines in Figure 2.a). Then, Z-shaped cells are defined (see the Z-shaped cell depicted in Figure 2.b), resulting in the truncated regular tetrahedral tensegrity. Rhombic cells can also be defined (one for each strut) removing and adding some cables as can be seen in Figure 2.c, where only a rhombic cell has been represented for the sake of clarity. In a similar way, Z-shaped cells of Figure 2.b can be replaced by X-rhombic cells (see Figure 2.d). It can be clearly seen in Figure 2.b, 2.c and 2.d that the cables of the elementary cells can be classified into three types: type-1 (red lines), type-2 (blue lines) and type-3 (green lines). The determination of feasible grouping of elements (like type-1, -2 and -3 of cables) is of great importance in the design of tensegrity structures using analytical form-finding methods.

In applying an analogous procedure, rhombic truncated tetrahedral, cubic, octahedral, dodecahedral and icosahedral tensegrities can be obtained (see (Zhang et al., 2013)).

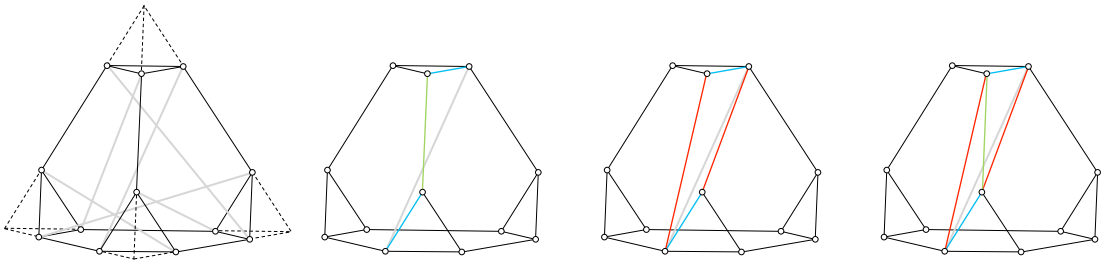

Figure 2. (a) Truncated regular tetrahedron and connection of the struts, (b) zigzag pattern, (c) rhombic pattern and (d) X-rhombic pattern. In (b), (c) and (d) only an elementary cell is drawn. Red, blue, green and grey lines correspond to type-1 cables, type-2 cables, type-3 cables and struts, respectively. (For interpretation of the references to color in this figure legend, the reader is referred to the web version of this article).

2.3 The Octahedron family

A tensegrity family is a group of tensegrity structures that share a common connectivity pattern (Fernández-Ruiz et al., 2019a). It is considered that a tensegrity belongs to a

family if it has as folded forms all the lower members of the family. Three members of the Octahedron family are: the octahedron, the expanded octahedron and the double-expanded octahedron (Fernández-Ruiz et al., 2019a) (see Figure 3.a, 3.b and 3.c respectively). All the components of the Octahedron family are formed by the combination of rhombic cells.

It is interesting to remark that in the case of the three members of the Octahedron family (Fernández-Ruiz et al., 2019a) represented in Figure 3 only two different q values were considered: q_c for cables and q_b for bars or struts (black and grey lines respectively in Figure 3).

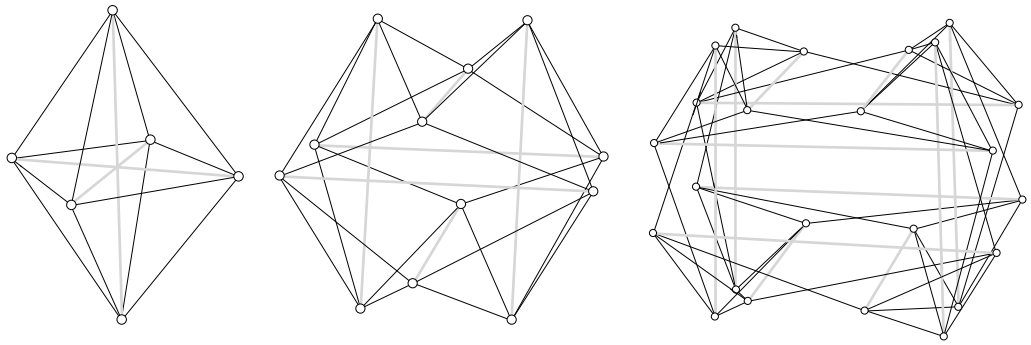

(a) (b) (c)

Figure 3. Octahedron family: (a) octahedron, (b) expanded octahedron and (c) double-expanded octahedron. Black lines correspond to cables and grey lines to struts.

New tensegrity forms can be derived from the Octahedron family based on its connectivity pattern, either by the definition of a higher member through an expansion process or by replacing their rhombic cells by other type of cells as in (Fernández-Ruiz et al., 2020). In addition, new equilibrium configurations of the members of the Octahedron family can be obtained by introducing a higher number of different force:length ratio values for cables and struts.

3. The X-Octahedron family: a new tensegrity family

All the members of the Octahedron family presented in (Fernández-Ruiz et al., 2019a)

were formed by rhombic cells. A new tensegrity family can be defined replacing the rhombic cells by another type of elementary cells. In (Fernández-Ruiz et al., 2020), rhombic cells were replaced by Z-shaped cells (see Figure 1.b), resulting in the so-called Z-Octahedron family. In this work, rhombic cells are replaced by X-rhombic cells (see Figure 1.c). In doing so, a new family of tensegrities is obtained: the so-called X-Octahedron family.

Relevant information about the self-equilibrium equations, the required rank deficiency and super-stability of the tensegrity structures studied in the work is collected in Appendix A.

3.1 The X-octahedron

A plane connection graph is a graphical representation of the connectivity between the nodes of a tensegrity (Fernández-Ruiz et al., 2019a). Figure 4.b shows the plane connection graph of the octahedron which has been defined based on the connectivity rules of the Octahedron family given in (Fernández-Ruiz et al., 2019a).

The plane connection graph of the X-octahedron was obtained replacing the rhombic cells of the octahedron by X-rhombic cells (see Figure 4.a). Three types of cables (type-1, type-2 and type-3) are identified following the pattern of the X-rhombic elementary cell depicted in Figure 2.d. Taking this into account, different element groupings can be chosen in order to obtain different equilibrium configurations of the X-octahedron.

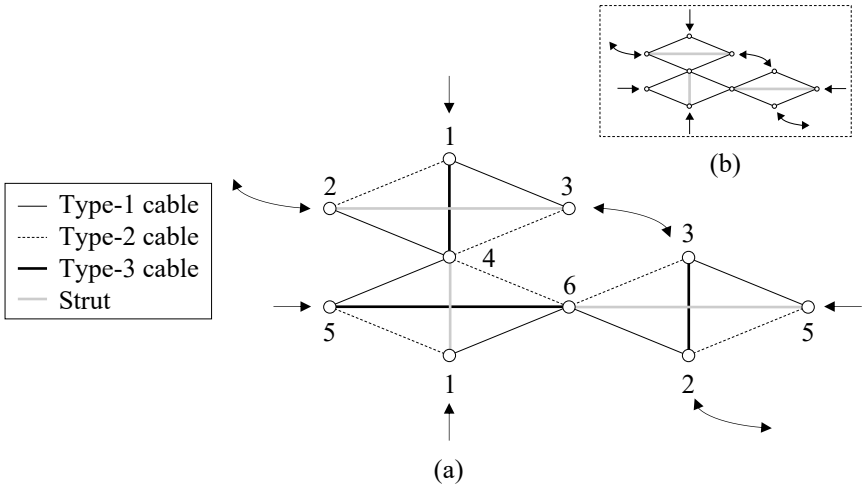

213

214 **Figure 4. (a) Plane connection graph of the X-octahedron and (b) of the octahedron (adapted from**
215 **(Fernández-Ruiz et al., 2019a)).**

216 ### 3.1.1 X-octahedron: two values of *q*

217 Firstly two values of q are going to be considered: q_{c1} for type-1, type-2 and type-3
218 cables and q_b for struts (see Figure 4.a). As in (Zhang et al., 2013), results are presented
219 as a function of an independent normalized force:length ratio taken as $Q_1 = -q_{c1}/q_b > 0$.
220 Once the characteristic polynomial $p(\lambda)$ of the resulting matrix **D** is computed, the
221 expressions of the polynomials that conforms the system of equations $\{a_1(Q_1) = 0, a_2$
222 $(Q_1) = 0, a_3(Q_1) = 0\}$ (see Eq. (A5)) are the ones shown in Eqs. (1), (2) and (3). As it is
223 explained in the Appendix, this system of equations implies that force density matrix **D**
224 has a rank deficiency of at least 4.

$$a_1 = 288Q_1^2\left(-1+3Q_1\right)^3 q_b^5 \tag{1}$$

$$a_2 = 48Q_1\left(1-3Q_1\right)^2\left(-2+15Q_1\right)q_b^4 \tag{2}$$

$$a_3 = 8\left(-1+3Q_1\right)\left(1+6Q_1\left(-4+15Q_1\right)\right)q_b^3 \tag{3}$$

225 The solution of the above system of equations is $\{Q_1 = 1/3\}$ which is super-stable
226 according to the conditions listed in the Appendix (see Figure 5 considering $q_{c1} = q_{c2} =$
227 q_{c3}). Other solutions different from $Q_1 = 1/3$ are discarded because they lead to negative
228 or null values of Q_1.

3.1.2 X-octahedron: three values of q

In this subsection three values of q are considered. The first element grouping adopted is: q_{c1} for type-1 and type-3 cables, q_{c2} for type-2 cables and q_b for struts (see Figure 4.a). The independent normalized force:length ratios taken as $Q_1 = -q_{c1}/q_b > 0$ and $Q_2 = -q_{c2}/q_b > 0$ are considered.

For this case, the solution that lead to $\{a_1\ (Q_1, Q_2) = 0, a_2\ (Q_1, Q_2) = 0, a_3\ (Q_1, Q_2) = 0\}$ (see Eq. (A5)) is $\{Q_1 = 1/3, Q_2 = 1/3\}$, which coincides with the solution of the previous case and that leads to a super-stable tensegrity structure (see Figure 5 considering $q_{c1} = q_{c2} = q_{c3}$).

Due to its length, from now on the expressions of the polynomials a_1, a_2 and a_3 of the tensegrities are not shown.

Nevertheless, others element groupings are possible. Let us consider the following element grouping: q_{c1} for type-1 and type-2 cables, q_{c2} for type-3 cables and q_b for struts (see Figure 4.a). For this case, the possible solutions of Eq. (A5) is collected in the expression $\{Q_2 = 1 - 2Q_1\}$, which corresponds to the self-equilibrated configurations of the X-octahedron considering three different values of q. However, it has to be pointed out that not all the $Q_1 – Q_2$ pairs satisfy the super-stability conditions listed in the Appendix.

For this case, a detailed study of the super-stability of the solution is carried out. For the rest of the tensegrities shown in this work, the super-stability study is presented in a summarized form.

First of all, the condition $q_b < 0$, $q_{c1} > 0$ and $q_{c2} > 0$ must be fulfilled (which corresponds to $Q_1 > 0$ and $Q_2 > 0$). This condition is fulfilled in the region $0 < Q_1 < 1/2$. Secondly, condition (i) for the super-stability of tensegrity structures requires that the force density matrix **D** must have exactly four zero-eigenvalues. This condition is fulfilled for all the

Q_1 - Q_2 pairs verifying $\{Q_2 = 1 - 2Q_1\}$ in the region $Q_1 > 0$ and $Q_2 > 0$. Thirdly, condition (ii) of super-stability requires that matrix **D** should be positive semi-definite. This condition is also fulfilled by the solution in the region $0 < Q_1 < 1/2$. Finally, condition (iii) requires that the geometry matrix **G** (defined in (Zhang and Ohsaki, 2015)) should have a rank of 6 in the case of a three-dimensional tensegrity. It can be proved that in this case just some $Q_1 – Q_2$ pairs fulfill the condition (iii) but they are not located in a particular region. The super-stability analysis is summarized in Table 1. In Table 1, if the checked condition is fulfilled by all the $Q_1 – Q_2$ pairs indicated in the first column, a tick is shown. On the contrary, if the studied condition is not fulfilled by all the $Q_1 – Q_2$ pairs, a cross is shown. If only a region of the studied solution fulfills a super-stability condition, it is defined explicitly in Table 1. The same shall apply for the rest of the tensegrities studied in this work.

Solution	**Q_1 and Q_2 > 0**	**Condition (i)**	**Condition (ii)**	**Condition (iii)**
$Q_2 = 1 - 2Q_1$	$0 < Q_1 < 1/2$	✓	✓	Irregular

Table 1. Super-stability analysis of the X-octahedron considering three values of *q*. Condition (i): force density matrix D has exactly four zero-eigenvalues. Condition (ii): matrix D is positive semi-definite. Condition (iii): geometry matrix G has a rank of 6.

The solution $Q_1 = Q_2 = 1/3$ is shown in Figure 5 (i.e., $q_{c1} = q_{c2} = q_{c3}$). This tensegrity is super-stable and coincides with the solution obtained in the previous case.

3.1.3 X-octahedron: four values of *q*

Finally, four values of q can be considered: q_{c1} for type-1 cables, q_{c2} for type-2 cables, q_{c3} for type-3 cables and q_b for struts (see Figure 4.a). In this case three independent normalized force:length ratios taken as $Q_1 = -q_{c1}/q_b > 0$, $Q_2 = -q_{c2}/q_b > 0$ and $Q_3 = -q_{c3}/q_b > 0$ are considered.

The solutions of Eq. (A5) for this case are $\{Q_1 = (1- Q_3)/2, Q_2 = (1- Q_3)/2\}$ and $\{Q_2 = Q_1, Q_3 = 1- 2Q_1\}$. As in the previous cases, solutions that lead to negative or null values

of the normalized force:length ratios are discarded. The stability of these tensegrities is analyzed in Table 2.

Solution	Q_1, Q_2 and $Q_3 > 0$	Condition (i)	Condition (ii)	Condition (iii)
$Q_1 = Q_2 = (1-Q_3)/2$	$0 < Q_3 < 1$	✓	✓	Irregular
$Q_2 = Q_1$ $Q_3 = 1-2Q_1$	$0 < Q_3 < 1/2$	✓	✓	Irregular

Table 2. Super-stability analysis of the X-octahedron considering four values of *q*. Condition (i): force density matrix D has exactly four zero-eigenvalues. Condition (ii): matrix D is positive semi-definite. Condition (iii): geometry matrix G has a rank of 6.

Figure 5 shows a super-stable equilibrium shape of the X-octahedron. The solutions listed in Table 2 leads to equilibrium shapes similar to the one shown in Figure 5.

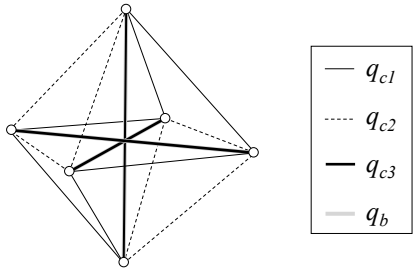

Figure 5. Equilibrium shape of the X-octahedron with $Q_1 = Q_2 = Q_3 = 1/3$ & $q_b = -1$.

3.2 The X-expanded octahedron

As in Section 3.1, the plane connection graph of the X-expanded octahedron was obtained replacing the rhombic cells of the expanded octahedron (see Figure 6.b) by X-rhombic cells (see Figure 6.a). It can be clearly seen that the X-expanded octahedron has twice the number of rhombic cells that the previous member of the family (the X-octahedron, see Figure 4.a). Consequently, the X-expanded octahedron has twice the number of nodes, cables and struts that the X-octahedron.

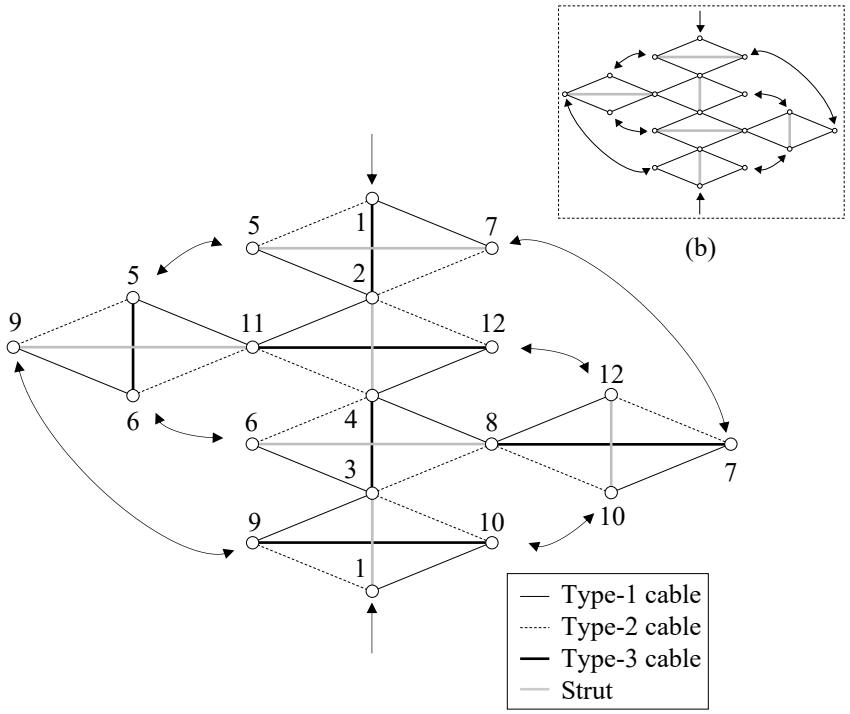

(a)

Figure 6. (a) Plane connection graph of the X-expanded octahedron and (b) of the expanded octahedron (adapted from (Fernandez-Ruiz et al., 2019a)).

3.2.1 X-expanded octahedron: two values of *q*

If two values of q are considered: q_{c1} for type-1, type-2 and type-3 cables and q_b for struts (see Figure 6.a), then the solutions of the system of equations in Eq. (A5) are $\{Q_1 = 1/3\}$ and $\{Q_1 = 3/5\}$. The tensegrity with $\{Q_1 = 1/3\}$ corresponds to the X-octahedron but with two nodes sharing the same position of the space (that is, duplicated nodes). This proves that the X-octahedron is the folded form of the X-expanded octahedron. This folded form is not super-stable. On the other hand, the solution $\{Q_1 = 3/5\}$ corresponds to the X-expanded octahedron (see Figure 7), which is super-stable.

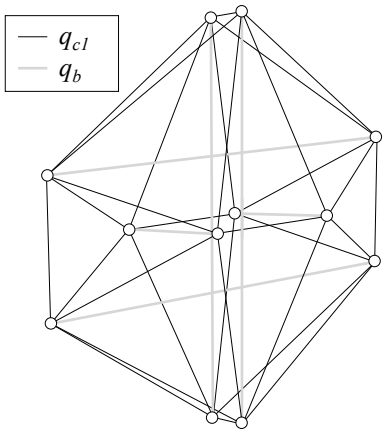

306

307 **Figure 7. Equilibrium shape of the X-expanded octahedron: Q_1 = 3/5 & q_b = -1.**

308 ### 3.2.2 X-expanded octahedron: three values of *q*

309 In this case two possible element groupings can be considered. The first alternative
310 consists on adopting the following values of q: q_{c1} for type-1 and type-2 cables, q_{c2} for
311 type-3 cables and q_b for struts (see Figure 6.a). The solutions that lead to $\{a_1 (Q_1, Q_2) =$
312 0, $a_2 (Q_1, Q_2) = 0$ and $a_3 (Q_1, Q_2) = 0\}$ in this case are the expressions shown in Eqs. (4)
313 and (5). Super-stability study is summarized in Table 3. Figure 8.a and .b show the
314 graphical representation of Eqs. (4) and (5) and the minimum eigenvalue of **D** for the Q_1
315 - Q_2 graph of Eq. (4) respectively for a better comprehension of Table 3.

$$Q_2 = 1 - 2Q_1 \tag{4}$$

$$Q_2 = \frac{2Q_1 - 3Q_1^2}{-1 + 2Q_1} \tag{5}$$

316

Solution	Q_1 and $Q_2 > 0$	Condition (i)	Condition (ii)	Condition (iii)
Eq. (4)	$0 < Q_1 < 1/2$	✓	×	-
Eq. (5)	$1/2 < Q_1 < 2/3$	✓	✓	✓

317 **Table 3. Super-stability analysis of the X-expanded octahedron considering three values of *q*.**
318 **Condition (i): force density matrix D has exactly four zero-eigenvalues. Condition (ii): matrix D is**
319 **positive semi-definite. Condition (iii): geometry matrix G has a rank of 6.**

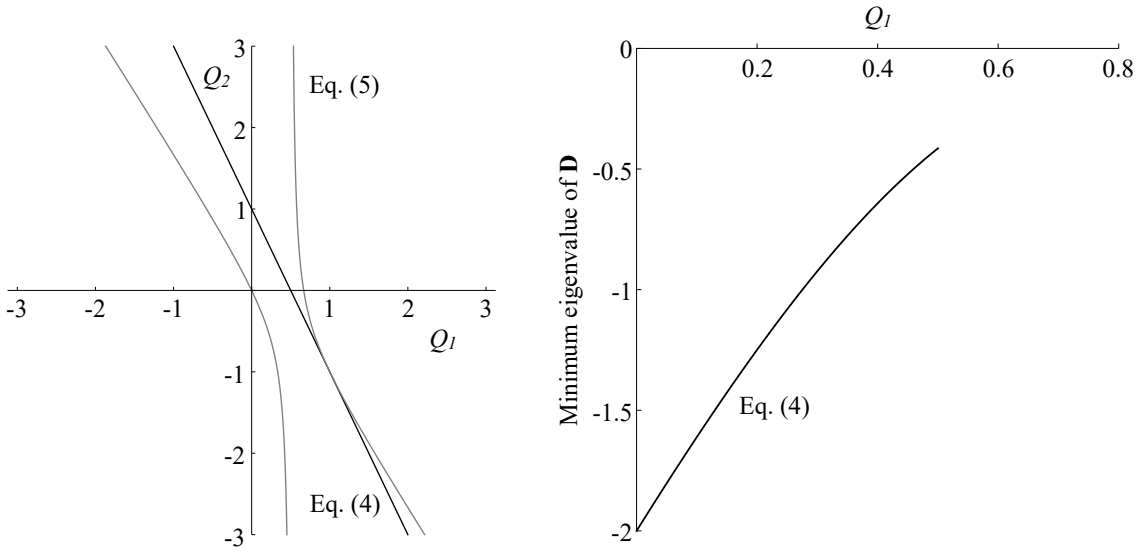

Figure 8. (a) Q_1 - Q_2 self-equilibrium graphs of the X-expanded octahedron (Eqs. (4) and (5)) and (b) minimum eigenvalue of D for the Q_1 - Q_2 graph of Eq. (4) in the region $Q_1 > 0$ and $Q_2 > 0$ considering $q_b = -1$.

As can be seen in Table 3, super-stable equilibrium configurations of the X-expanded octahedron are only obtained from Eq. (5) in the range indicated in Table 3 (see the example depicted in Figure 9).

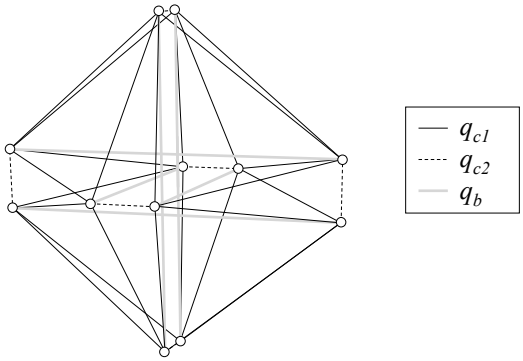

Figure 9. Equilibrium shape of the X-expanded octahedron: $Q_1 = 0.55$ & $Q_2 = 1.93$ (Eq. (5) & $q_b = -1$.

For the second possible grouping of elements , the following force-length ratios are imposed: q_{c1} for type-1 and type-3 cables, q_{c2} for type-2 cables and q_b for struts (see Figure 6.a). In this case the solutions of Eq. (A5) are $\{Q_1 = Q_2 = 1/3\}$ and the expressions shown in Eqs. (6) and (7). Super-stability study is summarized in Table 4.

$$Q_2 = \frac{-1+7Q_1-8Q_1^2-\sqrt{1-2Q_1-4Q_1^2+2Q_1^3+19Q_1^4}}{3\left(-1+3Q_1\right)} \tag{6}$$

$$Q_2 = \frac{-1+7Q_1-8Q_1^2+\sqrt{1-2Q_1-4Q_1^2+2Q_1^3+19Q_1^4}}{3\left(-1+3Q_1\right)} \tag{7}$$

333

Solution	Q_1 and $Q_2 > 0$	Condition (i)	Condition (ii)	Condition (iii)
$Q_1 = Q_2 = 1/3$	✓	✓	×	-
Eq. (6)	$0 < Q_1 < 1/10(11-\sqrt{41})$	✓	×	-
Eq. (7)	$1/3 < Q_1 < 1/10(11+\sqrt{41})$	✓	✓	✓

334 **Table 4. Super-stability analysis of the expanded X-octahedron considering three values of *q*.**
335 **Condition (i): force density matrix D has exactly four zero-eigenvalues. Condition (ii): matrix D is**
336 **positive semi-definite. Condition (iii): geometry matrix G has a rank of 6.**

337 Results in Table 4 show that super-stable tensegrity forms are only obtained from Eq.

338 (7) (see Figure 10).

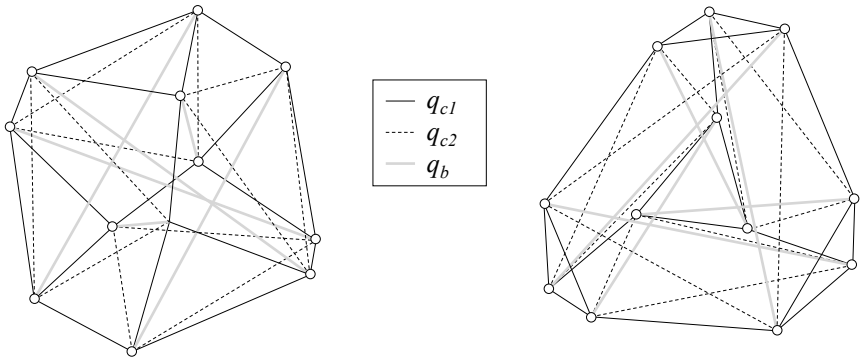

339 (a) (b)

340 **Figure 10. Equilibrium shapes of the X-expanded octahedron: (a) Q_1 = 0.7 & Q_2 = 0.51 (Eq. (7) & q_b**
341 **= -1 and (b) Q_1 = 1.6 & Q_2 = 0.06 (Eq. (7) & q_b = -1.**

342 ### 3.2.3 X-expanded octahedron: four values of *q*

343 Finally, four values of q are going to be considered: q_{c1} for type-1 cables, q_{c2} for type-2

344 cables, q_{c3} for type-3 cables and q_b for struts (see Figure 6.a). For this case, the solutions

345 of Eq. (A5) are the ones shown in Eqs. (8) and (9).

$$Q_3 = \frac{1}{4(-1+Q_1+Q_2)}\Big(-2+6Q_1-3Q_1^2+6Q_2-8Q_1Q_2-3Q_2^2- \\ \Big(4-8Q_1+8Q_1^2-12Q_1^3+9Q_1^4-8Q_2+8Q_1Q_2+4Q_1^2Q_2+8Q_2^2+ \\ 4Q_1Q_2^2-14Q_1^2Q_2^2-12Q_2^3+9Q_2^4\Big)^{1/2}\Big) \tag{8}$$

$$Q_3 = \frac{1}{4(-1+Q_1+Q_2)}\Big(-2+6Q_1-3Q_1^2+6Q_2-8Q_1Q_2-3Q_2^2+ \\ \Big(4-8Q_1+8Q_1^2-12Q_1^3+9Q_1^4-8Q_2+8Q_1Q_2+4Q_1^2Q_2+8Q_2^2+ \\ 4Q_1Q_2^2-14Q_1^2Q_2^2-12Q_2^3+9Q_2^4\Big)^{1/2}\Big) \tag{9}$$

Now Eqs. (8) and (9) do not correspond to curves as in the previous cases but to surfaces. In this case the super-stability analysis is a complex task and an individual analysis must be carried out for each triad (Q_1, Q_2, Q_3). Figure 11.a shows the graphical representation of Eq. (9). The Q_1 - Q_2 pairs that lead to a positive value of Q_3 can be seen in Figure 11.b.

Figure 12 shows several super-stable equilibrium configurations of the X-expanded octahedron obtained from Eq. (9).

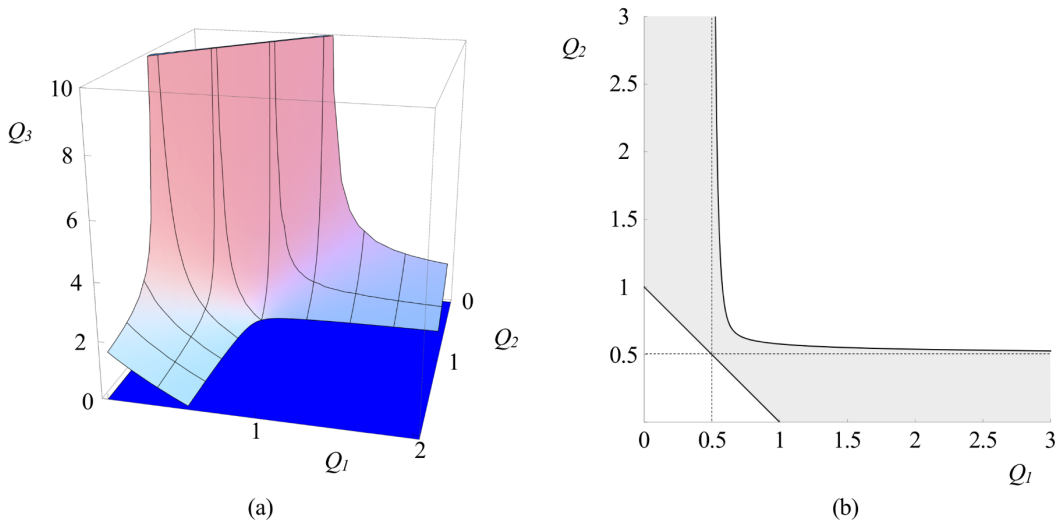

Figure 11. Graphical representation of Eq. (9) together with the plane $Q_1 = Q_2 = 0$ and (b) region of $Q_1 - Q_2$ pairs that leads to a positive value of Q_3 (grey area).

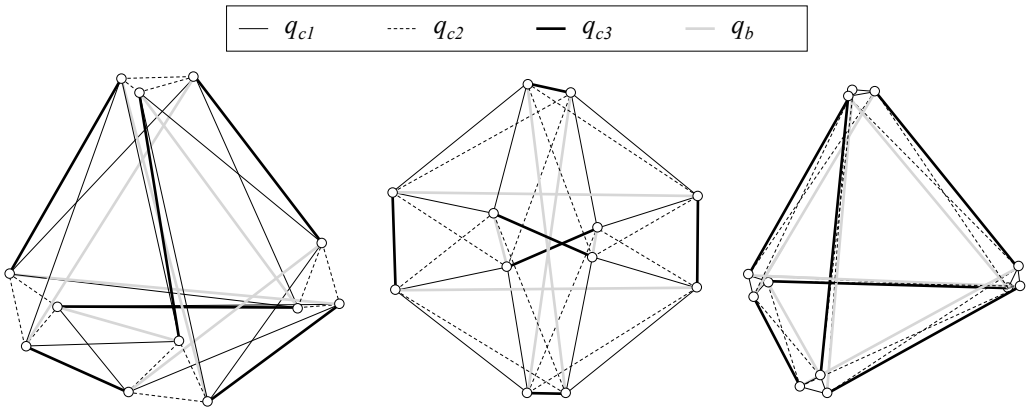

(a) (b) (c)

Figure 12. Equilibrium shapes of the X-expanded octahedron considering four different values of q: (a) $Q_1 = 1/4$, $Q_2 = 2$, $Q_3 = 0.752$ (Eq. (9)), $q_b = -1$, (b) $Q_1 = 0.7$, $Q_2 = 0.5$, $Q_3 = 0.773$ (Eq. (9)), $q_b = -1$ and (c) $Q_1 = 5$, $Q_2 = 1/4$, $Q_3 = 0.582$ (Eq. (9)), $q_b = -1$.

3.3 The X-double-expanded octahedron

As in the previous subsections, the plane connection graph of the X-double-expanded octahedron was obtained replacing the rhombic cells of the double-expanded octahedron (see Figure 13.b) by X-rhombic cells (see Figure 13.a). This tensegrity has twice the number of rhombic cells of the X-expanded octahedron (see Figure 6.a) and four times the number of rhombic cells of the octahedron (see Figure 4.a). The number of nodes, cables and struts follows the same proportionality rule.

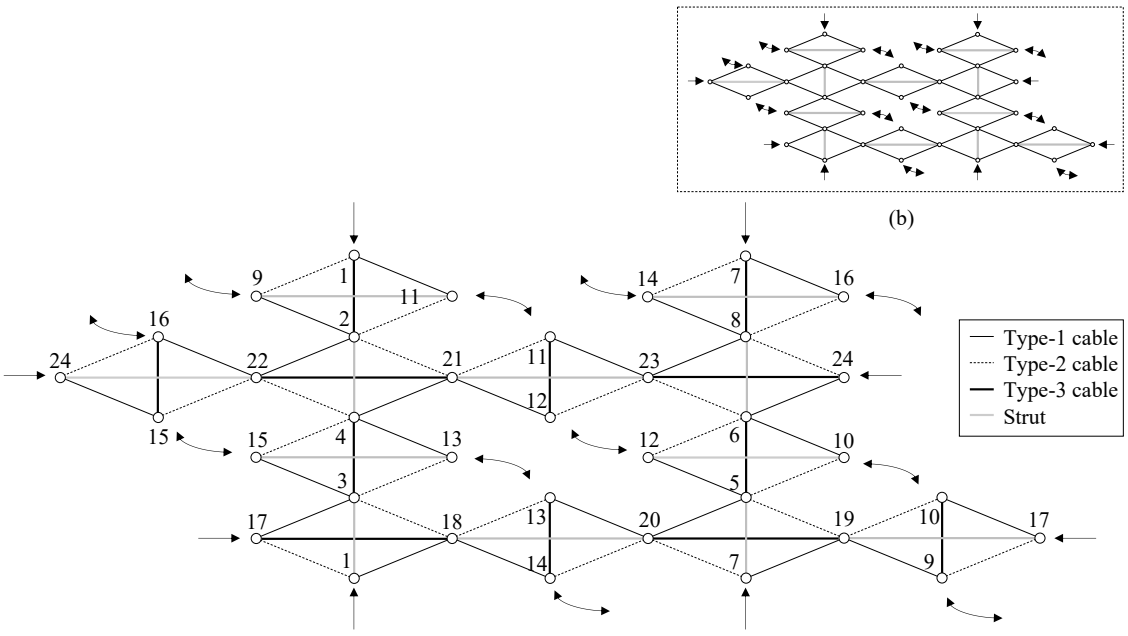

(a)

Figure 13. (a) Plane connection graph of the X-double-expanded octahedron and (b) of the double-expanded octahedron (adapted from (Fernandez-Ruiz et al., 2019a)).

3.3.1 X-double-expanded octahedron: two values of q

If two values of q are considered: q_{c1} for type-1, type-2 and type-3 cables and q_b for struts (see Figure 13.a), the solutions of Eq. (A5) are $\{Q_1 = 1/3\}$, $\{Q_1 = 3/5\}$ and $\{Q_1 = 5/7\}$. The solutions $\{Q_1 = 1/3\}$ and $\{Q_1 = 3/5\}$ correspond to the folded forms of the X-octahedron (members and nodes quadruplicated) and the X-expanded octahedron (members and nodes duplicated) respectively and both are not super-stable. Because all the self-equilibrium configurations of the previous members of the family are present as folded forms of the X-double-expanded octahedron, it can be concluded that all of them are members of a same tensegrity family. The solution $\{Q_1 = 5/7\}$ corresponds to the X-double-expanded octahedron, which is super-stable (Figure 14).

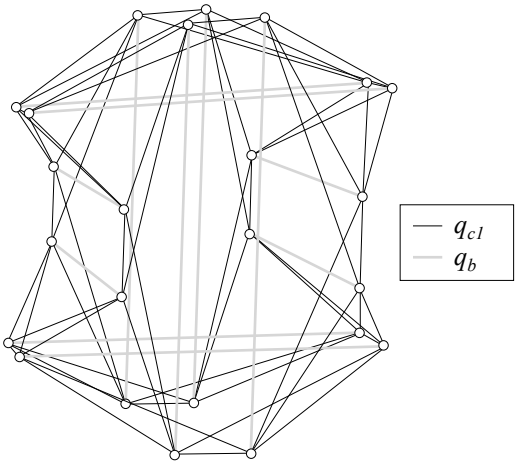

Figure 14. Equilibrium shape of the X-double-expanded octahedron: $Q_1 = 5/7$ & $q_b = -1$.

3.3.2 X-double-expanded octahedron: three values of q

As in Subsection 3.2.2, two possible element grouping can be considered. In the first one the values adopted for q are: q_{c1} for type-1 and type-2 cables, q_{c2} for type-3 cables and q_b for struts (see Figure 13.a). The solutions of Eq. (A5) are the expressions shown in Eqs. (4), (5) and (10). The study of the super-stability is summarized in Table 5.

$$Q_2 = \frac{3Q_1 - 4Q_1^2}{-2 + 3Q_1} \tag{10}$$

387

Solution	Q_1 and $Q_2 > 0$	Condition (i)	Condition (ii)	Condition (iii)
Eq. (4)	$0 < Q_1 < 1/2$	×	-	-
Eq. (5)	$1/2 < Q_1 < 2/3$	✓	×	-
Eq. (10)	$2/3 < Q_1 < 3/4$	✓	✓	✓

388 **Table 5. Super-stability analysis of the X-double-expanded octahedron considering three values of *q*.**
389 **Condition (i): force density matrix D has exactly four zero-eigenvalues. Condition (ii): matrix D is**
390 **positive semi-definite. Condition (iii): geometry matrix G has a rank of 6.**

391 A super-stable equilibrium shape of the X-double-expanded octahedron (obtained from
392 Eq. (10)) is depicted in Figure 15.

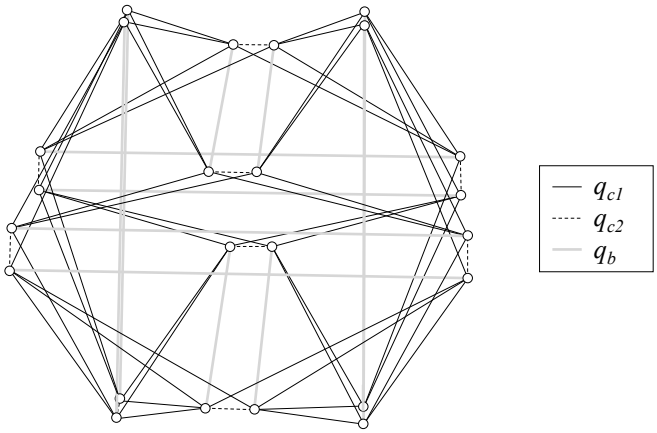

393

394 **Figure 15. Equilibrium shape of the X-double-expanded octahedron: Q_1 = 0.69 & Q_2 = 2.37 (Eq. (10)**
395 **& q_b = -1.**

396 The second possible grouping of elements corresponds to: q_{c1} for type-1 and type-3
397 cables, q_{c2} for type-2 cables and q_b for struts (see Figure 13.a). For this relationship
398 between the force-length ratios, the solutions of Eq. (A5) are $\{Q_1 = Q_2 = 1/3\}$ and the
399 expressions shown in Eqs. (6), (7) and (11). The super-stability is studied in Table 6.

$$Q_2 = \frac{7Q_1 - 5Q_1^2}{3\left(-1 + 3Q_1\right)} \tag{11}$$

400

Solution	Q_1 and $Q_2 > 0$	Condition (i)	Condition (ii)	Condition (iii)
$Q_1 = Q_2 = 1/3$	✓	×	-	-
Eq. (6)	$0 < Q_1 < 1/10(11-\sqrt{41})$	✓	×	-
Eq. (7)	$1/3 < Q_1 < 1/10(11+\sqrt{41})$	✓	$1 < Q_1 < 1/10(11+\sqrt{41})$	✓
Eq. (11)	$1/3 < Q_1 < 7/5$	✓	$1/3 < Q_1 < 1$	✓

Table 6. Super-stability analysis of the X-double-expanded octahedron considering three values of *q*. Condition (i): force density matrix D has exactly four zero-eigenvalues. Condition (ii): matrix D is positive semi-definite. Condition (iii): geometry matrix G has a rank of 6.

In this case a super-stable equilibrium shape of a folded form is obtained (Eq. (7), see Figure 16.a). Super-stable full forms are obtained using Eq. (11) if the values of Q_1 are in range indicated in Table 6 (see Figure 16.b).

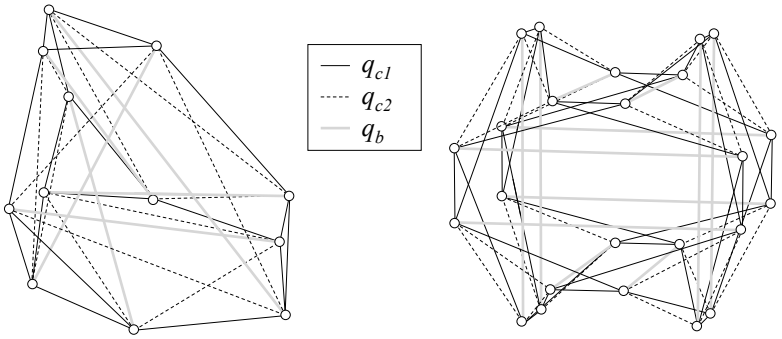

(a) (b)

Figure 16. Equilibrium shapes of the X-double-expanded octahedron considering three different values of *q*: (a) $Q_1 = 1.4$ & $Q_2 = 0.15$ (Eq. (7)) & $q_b = -1$ and (b) $Q_1 = 2/3$ & $Q_2 = 0.81$ (Eq. (11)) & $q_b = -1$.

3.3.3 X-double-expanded octahedron: four values of *q*

Finally, four values of q are going to be considered: q_{c1} for type-1 cables, q_{c2} for type-2 cables, q_{c3} for type-3 cables and q_b for struts (see Figure 13.a). For this case, the solutions of Eq. (A5) are $\{Q_1 = 1; Q_2 = 1/3\}$, $\{Q_2 = Q_1; Q_3 = 1\text{-}2\ Q_1\}$ and the expressions shown in Eqs. (8), (9), (12), (13) and (14).

$$Q_3 = \frac{3Q_1 - 2Q_1^2 + 3Q_2 - 6Q_1Q_2}{-4 + 3Q_1 + 3Q_2} \tag{12}$$

$$\left\{Q_2=\frac{1}{3}\left(2-\sqrt{-4+4Q_1+Q_1^2}\right);\ Q_3=\frac{1}{2}\left(-Q_1+\sqrt{-4+4Q_1+Q_1^2}\right)\right\} \tag{13}$$

$$\left\{Q_2=\frac{1}{3}\left(2+\sqrt{-4+4Q_1+Q_1^2}\right);\ Q_3=\frac{1}{2}\left(-Q_1-\sqrt{-4+4Q_1+Q_1^2}\right)\right\} \tag{14}$$

As in Subsection 3.2.3, the super-stability analysis of the tensegrities requires an individual study of each triad (Q_1, Q_2 ,Q_3) in Eqs. (12), (13) and (14). Figure 17 shows a super-stable shape of the X-double-expanded octahedron using Eq. (12).

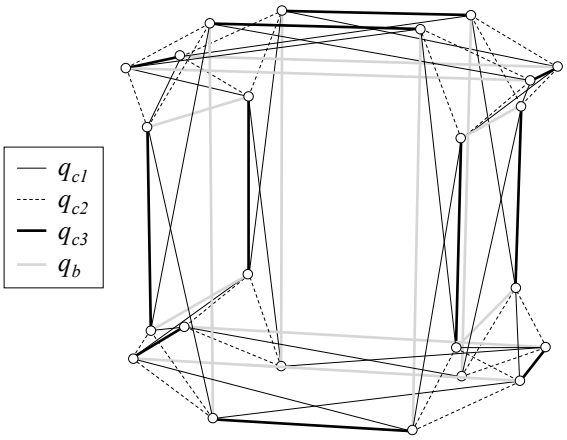

Figure 17. Equilibrium shape of the X-double-expanded octahedron considering four different values of q: Q_1 = 0.3 & Q_2 = 2 & Q_3 = 1.08 (Eq. (12)) & q_b = -1.

6. Conclusions

The Octahedron family has been presented as a new source of tensegrity families. The members of the Octahedron family are the octahedron, the expanded octahedron and the double-expanded octahedron. The topology of these tensegrity structures is stablished following a certain connectivity pattern, which is common for the whole family.

A new tensegrity family has been presented: the X-Octahedron family. The origin of the new family is the Octahedron family. Based on the cell substitution design method, rhombic cells of the Octahedron family have been replaced by X-rhombic cells, resulting in new tensegrity structures. The X-Octahedron family is composed by the X-octahedron, the X-expanded octahedron and the X-double-expanded octahedron. The X-

433 double-expanded octahedron contains as folded forms both the X-expanded octahedron
434 and the X-octahedron, which is a necessary condition for tensegrity families. Super-
435 stable tensegrity forms of the X-Octahedron family have been obtained analytically.
436 Several element groupings have been considered in order to obtain different equilibrium
437 configurations of the members of the new family. It has been proved that tensegrity
438 families can be a good source of new tensegrity forms.
439

440 **Appendix A. Self-equilibrium, rank deficiency and super-stability of tensegrity**
441 **structures**

442 **A.1 Self-equilibrium of tensegrity structures**

443 The FDM introduced in (Schek, 1974) is a form finding method for general networks.
444 The equilibrium of a mesh with n free nodes, n_f fixed nodes and m members is obtained
445 considering constant values of force:length ratio to each member of the mesh. Free
446 nodes are free to move in the space, while fixed nodes act as supports. The force:length
447 ratio or force density q_j *of* the jth member is defined as the ratio between the axial force
448 and the length of the member jth of the mesh. The connectivity matrix $\mathbf{C_S}$ ($\in \Re^{m\times(n+nf)}$)
449 shows the connectivity between the nodes of the mesh; it can be easily defined based on
450 topological rules as described in (Hernández-Montes et al., 2006). The connectivity
451 matrix is constructed in the following way: if a general member j connects nodes i and k
452 (with $i < k$), the ith and kth elements of the jth row of $\mathbf{C_S}$ are set to 1 and -1 respectively
453 (see Eq. (A1)).

$$\mathbf{C_S}(j,r) = \begin{cases} +1 & \text{if } i(j) = r \\ -1 & \text{if } k(j) = r \\ 0 & \text{otherwise} \end{cases} \tag{A1}$$

454 As it is proposed by Schek (Schek, 1974), $\mathbf{C_S}$ can be partitioned into two matrices $\mathbf{C}$
455 ($\in \Re^{m\times n}$) and $\mathbf{C_f}$ ($\in \Re^{m\times nf}$) if the fixed nodes are numbered first ($\mathbf{C_S} = [\mathbf{C}\ \mathbf{C_f}]$). Let us

denote $\mathbf{x}$, $\mathbf{y}$, $\mathbf{z}$ ($\in\Re^{n}$) and $\mathbf{x_f}$, $\mathbf{y_f}$, $\mathbf{z_f}$ ($\in\Re^{nf}$) as the nodal coordinate vectors in x, y and z directions of free and fixed nodes respectively. The external forces applied at the free nodes in the x, y and z directions are collected in the vectors $\mathbf{P_x}$, $\mathbf{P_y}$ and $\mathbf{P_z}$ ($\in\Re^{n}$) respectively. Then, the equilibrium equations of a general pin-jointed network are shown in Eq. (A2) as proposed in (Schek, 1974).

$$\begin{aligned}\mathbf{C}^{\mathrm{T}}\mathbf{QCx}+\mathbf{C}^{\mathrm{T}}\mathbf{QC_f x_f} &= \mathbf{P_x}\\ \mathbf{C}^{\mathrm{T}}\mathbf{QCy}+\mathbf{C}^{\mathrm{T}}\mathbf{QC_f y_f} &= \mathbf{P_y}\\ \mathbf{C}^{\mathrm{T}}\mathbf{QCz}+\mathbf{C}^{\mathrm{T}}\mathbf{QC_f z_f} &= \mathbf{P_z}\end{aligned} \tag{A2}$$

In Eq. (A2) $\mathbf{Q}$ ($\in\Re^{m\times m}$) is the diagonal square matrix of the vector $\mathbf{q}$ ($\in\Re^{m}$) that contains the force:length ratio of each branch. The symbol $[]^{\mathrm{T}}$ represents the transpose operation of a matrix or vector.

In tensegrity structures external forces are ignored (self-stressed equilibrium) and fixed nodes are not required because they are free-standing structures (n_f=0). In this context, the equilibrium equations of a general tensegrity can be formulated as:

$$\begin{aligned}\mathbf{D\,x} &= 0\\ \mathbf{D\,y} &= 0\\ \mathbf{D\,z} &= 0\end{aligned} \tag{A3}$$

where $\mathbf{D} = \mathbf{C}^{\mathrm{T}}\mathbf{QC}$ ($\in\Re^{n\times n}$) is the force density matrix.

A.2 Rank deficiency

In the case of tension (Hernández-Montes et al., 2006) and compression (Fernández-Ruiz et al., 2017) structures where the force:length ratio values of all the members of the mesh are of the same sign ($q > 0$ in tension and $q < 0$ in compression) and fixed nodes are present, the form-finding problem is well-solved (Levy and Spillers, 2004) because its corresponding matrix $\mathbf{D}$ is nonsingular. Therefore, $\mathbf{D}$ can be inverted and the positions of the free nodes are computed solving Eq. (A2). In the case of compression structures with prestressing tendons, some additional conditions must be fulfilled in the

476 determination of an equilibrium configuration (Fernández-Ruiz et al., 2019c).
477 In the case of tensegrity structures, tension (cables) and compression (struts) members
478 coexist. By construction of **D**, the sum of the elements of each row or a column is zero.
479 Consequently, **D** is always singular and the equilibrium configuration is not obtained
480 directly from Eq. (A3) as in both compression and tension structures. It can be proved
481 that a tensegrity of dimension *d* has a force density matrix with a rank deficiency of at
482 least *d+1* (Hernández-Montes et al., 2018; Zhang and Ohsaki, 2006) (non-degeneracy
483 condition). This condition is achieved imposing that the characteristic polynomial (see
484 Eq. (A4)) corresponding to the force density matrix has $d + 1$ zero roots. Consequently,
485 coefficients a_3, a_2, a_1 and a_0 of the characteristic polynomial must be zero in order to
486 obtain a three-dimensional (3D) tensegrity. As matrix **D** is always singular, coefficient
487 a_0 is always 0. So, if the three coefficients a_3, a_2 and a_1 are set to zero a system of
488 polynomial equations in terms of the force:length ratios of the members of the 3D
489 tensegrity is provided. This system of equations can be solved analytically if some
490 relations between the force:length ratio of the members are imposed (Fernández-Ruiz et
491 al., 2019a; Hernández-Montes et al., 2018; Zhang et al., 2013) (see Eq. (A5)).

$$p(\lambda)=\lambda^n+a_{n-1}\lambda^{n-1}+\ldots+a_1\lambda+a_0 \tag{A4}$$

$$\begin{aligned} a_3(q_1,\ldots,q_m) &= 0 \\ a_2(q_1,\ldots,q_m) &= 0 \\ a_1(q_1,\ldots,q_m) &= 0 \end{aligned} \tag{A5}$$

492 A more detailed description of the analytical form-finding procedure used in this work
493 can be seen in (Fernández-Ruiz et al., 2019a; Hernández-Montes et al., 2018).

494 **A.3 Super-stability of tensegrity structures**

495 A tensegrity which is always stable, regardless of material properties and prestress, is
496 called super-stable (Connelly, 1998; Zhang and Ohsaki, 2007). The super-stability
497 conditions of tensegrities are the following (Connelly, 1998; Zhang and Ohsaki, 2015,

498 2007):

499 i. The rank deficiency of the force density matrix **D** is exactly $d + 1$.

500 ii. The force density matrix **D** is positive semi-definite.

501 iii. The rank of the matrix **G**, defined in Eq. (A6) is $(d^2 + d)/2$.

$$\mathbf{G} = \left(\mathbf{Uu}, \mathbf{Vv}, \mathbf{Ww}, \mathbf{Uv}, \mathbf{Uw}, \mathbf{Vw}\right) \tag{A6}$$

502 Matrix **G** is called the geometry matrix because it is only related to the geometry of the
503 structure. A deeper explanation about matrix **G** can be seen in (Zhang and Ohsaki,
504 2015). The stability of tensegrity structures has been discussed in detail in (Fernández-
505 Ruiz et al., 2019a; Zhang and Ohsaki, 2015, 2007).

506

507 **References**

508 Aloui, O., Flores, J., Orden, D., Rhode-Barbarigos, L., 2019. Cellular morphogenesis of
509 three-dimensional tensegrity structures. Comput. Methods Appl. Mech. Eng. 346,
510 85–108. https://doi.org/10.1016/j.cma.2018.10.048

511 Aloui, O., Orden, D., Rhode-Barbarigos, L., 2018. Generation of planar tensegrity
512 structures through cellular multiplication. Appl. Math. Model. 64, 71–92.
513 https://doi.org/10.1016/j.apm.2018.07.024

514 Bel Hadj Ali, N., Rhode-Barbarigos, L., Smith, I.F.C., 2011. Analysis of clustered
515 tensegrity structures using a modified dynamic relaxation algorithm. Int. J. Solids
516 Struct. 48, 637–647. https://doi.org/10.1016/j.ijsolstr.2010.10.029

517 Connelly, R., 1998. Tensegrity structures. Why are they stable?, in: Thorpe, M.F.,
518 Duxbury, P.M. (Eds.), Rigidity Theory and Applications. Kluwer Academic /
519 Plenum Publishers, pp. 47–54.

520 Connelly, R., Back, A., 1998. Mathematics and tensegrity. Am. Sci. 86, 142–151.
521 https://doi.org/10.1511/1998.2.142

522 Estrada, G.G., Bungartz, H.-J., Mohrdieck, C., 2006. Numerical form-finding of
523 tensegrity structures. Int. J. Solids Struct. 43, 6855–6868.
524 Estrada, G.G., Bungartz, H.-J., Mohrdieck, C., 2005. On cylindrical tensegrity
525 structures, in: Proceedings of the 5th International Conference on Computation of
526 Shell and Spatial Structures.
527 Feng, X., Guo, S., 2015. A novel method of determining the sole configuration of
528 tensegrity structures. Mech. Res. Commun. 69, 66–78.
529 https://doi.org/10.1016/j.mechrescom.2015.06.012
530 Feng, X.Q., Li, Y., Cao, Y.P., Yu, S.W., Gu, Y.T., 2010. Design methods of rhombic
531 tensegrity structures. Acta Mech. Sin. Xuebao 26, 559–565.
532 https://doi.org/10.1007/s10409-010-0351-6
533 Fernández-Ruiz, M.A., Hernández-Montes, E., Carbonell-Márquez, J.F., Gil-Martín,
534 L.M., 2019a. Octahedron family: The double-expanded octahedron tensegrity. Int.
535 J. Solids Struct. 165, 1–13. https://doi.org/10.1016/j.ijsolstr.2019.01.017
536 Fernández-Ruiz, M.A., Hernández-Montes, E., Carbonell-Márquez, J.F., Gil-Martín,
537 L.M., 2019b. Form finding of tensegrity structures based on families: the
538 octahedron family, in: 5th International Conference on Mechanical Models in
539 Structural Engineering. Alicante (Spain).
540 Fernández-Ruiz, M.A., Hernández-Montes, E., Carbonell-Márquez, J.F., Gil-Martín,
541 L.M., 2017. Patterns of force:length ratios for the design of compression structures
542 with inner ribs. Eng. Struct. 148, 878–889.
543 https://doi.org/10.1016/j.engstruct.2017.07.027
544 Fernández-Ruiz, M.A., Hernández-Montes, E., Gil-Martín, L.M., 2020. The Z-
545 octahedron family: A new tensegrity family. Eng. Struct. 222.
546 https://doi.org/10.1016/j.engstruct.2020.111151

547 Fernández-Ruiz, M.A., Moskaleva, A., Gil-Martín, L.M., Palomares, A., Hernández-
548 Montes, E., 2019c. Design and form- finding of compression structures with
549 prestressing tendons. Eng. Struct. 197, 109394.
550 https://doi.org/10.1016/j.engstruct.2019.109394
551 Fuller, R.B., 1975. Synergetics - explorations in the geometry of thinking. Macmillan,
552 London, UK.
553 Graells Rovira, A., Mirats Tur, J.M., 2009. Control and simulation of a tensegrity-based
554 mobile robot. Rob. Auton. Syst. 57, 526–535.
555 https://doi.org/10.1016/j.robot.2008.10.010
556 Hernández-Montes, E., Fernández-Ruiz, M.A., Gil-Martín, L.M., Merino, L., Jara, P.,
557 2018. Full and folded forms: a compact review of the formulation of tensegrity
558 structures. Math. Mech. Solids 23, 944–949.
559 https://doi.org/10.1177/1081286517697372
560 Hernández-Montes, E., Jurado-Piña, R., Bayo, E., 2006. Topological Mapping for
561 Tension Structures. J. Struct. Eng. 132, 970–977.
562 https://doi.org/10.1061/(ASCE)0733-9445(2006)132:6(970)
563 Ingber, D.E., 2003. Tensegrity I. Cell structure and hierarchical systems biology. J. Cell
564 Sci. 116, 1157–1173. https://doi.org/10.1242/jcs.00359
565 Ingber, D.E., 1993. Cellular tensegrity: defining new rules of biological design that
566 govern the cytoskeleton. J. Cell Sci. 104 (Pt 3, 613–27.
567 Levy, R., Spillers, W.R., 2004. Analysis of geometrically nonlinear structures, 2nd Ed.
568 ed. Chapman & Hall, London.
569 Li, Y., Feng, X.Q., Cao, Y.P., Gao, H., 2010. Constructing tensegrity structures from
570 one-bar elementary cells. Proc. R. Soc. A Math. Phys. Eng. Sci. 466, 45–61.
571 https://doi.org/10.1098/rspa.2009.0260

572 Linkwitz, K., Schek, H.J., 1971. Einige Bemerkungen zur Berechnung von
573 vorgespannten Seilnetzkonstruktionen. Ingenieur-Archiv. 40, 145–158.
574 https://doi.org/10.1007/BF00532146
575 Maina, J.N., 2007. Spectacularly robust! Tensegrity principle explains the mechanical
576 strength of the avian lung. Respir. Physiol. Neurobiol. 155, 1–10.
577 https://doi.org/https://doi.org/10.1016/j.resp.2006.05.005
578 Masic, M., Skelton, R.E., Gill, P.E., 2005. Algebraic tensegrity form-finding. Int. J.
579 Solids Struct. 42, 4833–4858. https://doi.org/10.1016/j.ijsolstr.2005.01.014
580 Micheletti, A., Williams, W.O., 2007. A marching procedure for form-finding for
581 tensegrity structures. J. Mech. Mater. Struct. 2, 857–882.
582 https://doi.org/10.2140/jomms.2007.2.857
583 Motro, R., 1984. Forms and forces in tensegrity systems, in: Nooshin, H. (Ed.),
584 Proceedings of Third International Conference on Space Structures. Elsevier,
585 Amsterdam, pp. 180–185.
586 Nishimura, Y., Murakami, H., 2001. Initial shape-finding and modal analyses of cyclic
587 frustum tensegrity modules. Comput. Methods Appl. Mech. Eng. 190, 5795–5818.
588 https://doi.org/10.1016/S0045-7825(01)00198-0
589 Otter, J.R.H., 1965. Computations for prestressed concrete reactor pressure vessels
590 using dynamic relaxation. Nucl. Struct. Eng. 1, 61–75.
591 https://doi.org/10.1016/0369-5816(65)90097-9
592 Pugh, A., 1976. An introduction to tensegrity. University of California Press.
593 Rhode-Barbarigos, L., Hadj Ali, N.B., Motro, R., Smith, I.F.C., 2010. Designing
594 tensegrity modules for pedestrian bridges. Eng. Struct. 32, 1158–1167.
595 https://doi.org/10.1016/j.engstruct.2009.12.042
596 Schek, H.J., 1974. The force density method for form-finding and computation of

general networks. Comput. Methods Appl. Mech. Eng. 3, 115–134. https://doi.org/10.1016/0045-7825(74)90045-0

Sultan, C., Corless, M., Skelton, R.E., 2001. The prestressability problem of tensegrity structures: Some analytical solutions. Int. J. Solids Struct. 38, 5223–5252. https://doi.org/10.1016/S0020-7683(00)00401-7

Tibert, A.G., Pellegrino, S., 2003. Review of Form-Finding Methods for Tensegrity Structures. Int. J. Sp. Struct. 18, 209–223. https://doi.org/10.1260/026635103322987940

Tibert, A.G., Pellegrino, S., 2002. Deployable Tensegrity Reflectors for Small Satellites. J. Spacecr. Rockets 39, 701–709. https://doi.org/10.2514/2.3867

Tran, H.C., Lee, J., 2010. Advanced form-finding of tensegrity structures. Comput. Struct. 88, 237–246. https://doi.org/10.1016/j.compstruc.2009.10.006

Vassart, N., Motro, R., 1999. Multiparameted form-finding method: application to tensegrity systems. Int. J. Sp. Struct. 14, 89–104.

Zhang, J., Ohsaki, M., 2013. Free-form design of tensegrity structures by non-rigid-body motion analysis, in: Proceedings of IASS Annual Symposia.

Zhang, J.Y., Guest, S.D., Ohsaki, M., 2009a. Symmetric prismatic tensegrity structures: Part I. Configuration and stability. Int. J. Solids Struct. 46, 1–14. https://doi.org/10.1016/j.ijsolstr.2008.08.032

Zhang, J.Y., Guest, S.D., Ohsaki, M., 2009b. Symmetric prismatic tensegrity structures. Part II: Symmetry-adapted formulations. Int. J. Solids Struct. 46, 15–30. https://doi.org/10.1016/j.ijsolstr.2008.07.035

Zhang, J.Y., Ohsaki, M., 2015. Tensegrity Structures. Form, Stability, and Symmetry. Springer.

Zhang, J.Y., Ohsaki, M., 2012. Self-equilibrium and stability of regular truncated

622 tetrahedral tensegrity structures. J. Mech. Phys. Solids 60, 1757–1770.
623 https://doi.org/10.1016/j.jmps.2012.06.001
624 Zhang, J.Y., Ohsaki, M., 2007. Stability conditions for tensegrity structures. Int. J.
625 Solids Struct. 44, 3875–3886. https://doi.org/10.1016/j.ijsolstr.2006.10.027
626 Zhang, J.Y., Ohsaki, M., 2006. Adaptive force density method for form-finding
627 problem of tensegrity structures. Int. J. Solids Struct. 43, 5658–5673.
628 https://doi.org/10.1016/j.ijsolstr.2005.10.011
629 Zhang, J.Y., Ohsaki, M., Tsuura, F., 2019. Self-equilibrium and super-stability of
630 truncated regular hexahedral and octahedral tensegrity structures. Int. J. Solids
631 Struct. 161, 182–192. https://doi.org/10.1016/j.ijsolstr.2018.11.017
632 Zhang, L.Y., Li, Y., Cao, Y.P., Feng, X.Q., 2013. A unified solution for self-
633 equilibrium and super-stability of rhombic truncated regular polyhedral
634 tensegrities. Int. J. Solids Struct. 50, 234–245.
635 https://doi.org/10.1016/j.ijsolstr.2012.09.024
636 Zhang, L.Y., Li, Y., Cao, Y.P., Feng, X.Q., Gao, H., 2012. Self-equilibrium and super-
637 stability of truncated regular polyhedral tensegrity structures: A unified analytical
638 solution. Proc. R. Soc. A Math. Phys. Eng. Sci. 468, 3323–3347.
639 https://doi.org/10.1098/rspa.2012.0260